

Supporting Information

Inserting an “Atomic Trap” for Directional Dopant Migration in Core/Multi-Shell Quantum Dots

Chun Chu,^a Elan Hofman,^a Chengpeng Gao,^a Shuya Li,^a Hanjie Lin,^a Walker MacSwain,^a John M. Franck,^a Robert W. Meulenberg,^a Arindam Chakraborty,^a Weiwei Zheng^{*,a}

a. Department of Chemistry, Syracuse University, Syracuse, New York 13244, United States. E-mail: wzhen104@syr.edu

b. Department of Physics and Astronomy and Frontier Institute for Research in Sensor Technologies, University of Maine, Orono, Maine 04469, United States.

Table of Contents

I. Experimental section.

II. Controlled *outward* dopant migration in Mn core-doped core/multi-shell QDs.

Figure S1. TEM images and histogram of selected (a and d) Mn:CdS core QDs, (b and e) Mn:CdS/CdZnS/ZnS_{4 MLs} core/multi-shell QDs, (c and f) Mn:CdS/ZnS_{5 MLs} core/shell QDs. The insets are the high-resolution TEM images showing d-spacing of the (111) lattice plane of the corresponding QDs.

Figure S2. (a) XRD patterns of Mn:CdS/ZnS core/shell QDs. (b) XRD analysis of full width at half maximum (FWHM) of the (111) diffraction peak of the Mn:CdS/ZnS and Mn:CdS/CdZnS/ZnS core/multi-shell QDs as a function of the shell thickness.

Table S1. The average distance between Mn ions inside Mn:CdS core QDs.

Table S2. The average distance between Mn ions inside Mn:CdS/CdZnS QDs and Mn:CdS/ZnS QDs with outward dopant migration behavior.

Figure S3. Room temperature X-band EPR spectra of Mn:CdS/ZnS_(1-5 MLs) core/shell QDs.

Figure S4. FWHM of Mn PL peak for Mn:CdS/ZnS_(1-5 MLs) and Mn:CdS/CdZnS/ZnS_(1-4 MLs) core/multi-shell QDs.

Figure S5. Schematic of inserting an alloyed CdZnS layer to reduce the lattice strain between CdS and ZnS lattice.

Figure S6. PL QYs of (a) undoped CdS/ZnS_(1-5 MLs) and doped Mn:CdS/ZnS_(1-5 MLs) core/multi-shell QDs without an inserted alloy dopant trap, and (b) undoped CdS/CdZnS/ZnS_(1-4 MLs) and doped Mn:CdS/CdZnS/ZnS_(1-4 MLs) core/multi-shell QDs with an inserted CdZnS alloy dopant trap as a function of ZnS monolayers, respectively.

III. Controlled *inward* dopant migration in Mn shell-doped core/multi-shell QDs.

Mn ion doping into ZnS shell with smaller initial substitutional Zn sites.

Figure S7. XRD patterns of CdS core and CdS/CdZnS/Mn:ZnS/ZnS_(1-5 MLs) core/multi-shell QDs.

Figure S8. Normalized absorption (dotted lines) and PL (solid lines) spectra of CdS core and CdS/CdZnS/Mn:ZnS/ZnS_(1-5 MLs) core/multi-shell QDs.

Mn ion doping into CdS shell with larger initial substitutional Cd sites.

Figure S9. TEM images and histogram of CdS/CdZnS/Mn:CdS and CdS/CdZnS/Mn:CdS/ZnS_{5 MLs} core/multi-shell QDs.

Figure S10. XRD patterns of CdS/CdZnS/Mn:CdS/ZnS core/multi-shell QDs.

Table S3. The average distance between Mn ions inside CdS/CdZnS/Mn:CdS QDs and CdS/CdZnS/Mn:CdS/ZnS QDs with inward dopant migration behavior.

Scheme S1. Average Mn-Mn distance before and after both outward and inward dopant migration inside core- and shell-doped QDs, respectively.

Figure S11. TEM images and histogram of CdS/CdS/Mn:CdS and CdS/CdS/Mn:CdS/ZnS_{5 MLs} core/multi-shell QDs.

Figure S12. XRD patterns of CdS/CdS/Mn:CdS/ZnS core/multi-shell QDs.

Figure S13. Room temperature X-Band EPR spectra of CdS/CdS/Mn:CdS/ZnS_(1-5 MLs) core/multi-shell QDs.

Figure S14. Normalized absorption (dotted lines) and PL (solid lines) spectra of (a) CdS/CdZnS/Mn:CdS/ZnS_(1-5 MLs) and (b) CdS/CdS/Mn:CdS/ZnS_(1-5 MLs) core/multi-shell QDs.

Figure S15. PL QYs (a) shell doped CdS/CdZnS/Mn:CdS/ZnS_(1-5 MLs) and undoped CdS/CdZnS/CdS/ZnS_(1-5 MLs) core/multi-shell QDs, and (b) shell doped CdS/CdS/Mn:CdS/ZnS_(1-5 MLs) and undoped CdS/CdS/CdS/ZnS_(1-5 MLs) core/multi-shell QDs.

I. Experimental section.

Chemicals.

Cd(NO₃)₂·4H₂O (≥99.0%, Sigma-Aldrich), Mn(CH₃CO₂)₂ (>98%, Alfa Aesar), sulfur powder (99.998%, Sigma-Aldrich), cadmium oxide (99.99%, Sigma-Aldrich), zinc oxide (≥99.0%, Sigma-Aldrich), HNO₃ (65%, Fisher), oleylamine (OAm, 70%, Sigma-Aldrich), 1-dodecanethiol (DDT, ≥98%, Sigma-Aldrich), oleic acid (OA, 90%, Sigma-Aldrich), 1-octadecene (ODE, 90%, Alfa Aesar), toluene (≥99.5%, Fisher), acetone (≥99.5%, Fisher), ethanol (≥99.5%, VWR), and hexane (>98%, Alfa Aesar) were used as received.

Stock solutions.

(1) Sulfur precursors.

a) *Sulfur-OAm solution for the synthesis of the CdS core QDs.* 19.5 mg (0.6 mmol) sulfur powder was added into a three-neck flask containing 3 mL OAm. The solution was degassed for 30 minutes at room temperature and then heated to 100 °C under Argon (Ar) and kept stirring at 100 °C for about 3 hours. Then the solution was cooled to room temperature and reheated before injection.^{1,2}

b) *Sulfur-ODE solution for the synthesis of metal sulfide shells (i.e., CdS, ZnS, and CdZnS shell).* 32.0 mg (1.0 mmol) sulfur powder was added into a vial which contained 10 mL ODE. The solution was degassed for 30 minutes at room temperature and sonicated at least 2 hours after refilling with Ar.^{1,2}

(2) Zn precursor for the growth of ZnS shell. 81.5 mg (1.0 mmol) zinc oxide was mixed with 9 mL ODE and 1 mL OA in a three-neck flask. After degassing for 1 hour at 100 °C, the solution was heated to 310 °C under Ar. Cooled the solution to the room temperature after it was completely clearly. Reheated the solution to a clear solution before the injection.^{1,2}

(3) Cd/Zn precursor for the growth of CdZnS alloyed shell. 32.0 mg (0.25 mmol) cadmium oxide and 20.3 mg (0.25 mmol) zinc oxide were dissolved in 3.6 mL ODE and 1.25 g OA. After degassing for 1 hour at 100 °C, the solution was heated to 310 °C under Ar. After the solution turned clear, the solution was cooled to room temperature.¹ Reheated the solution to a clear solution before the injection.

(4) Cd precursor for the growth of CdS shell. 32.0 mg (0.25 mmol) cadmium oxide was dissolved in 1.8 mL ODE and 0.62 g OA. After degassing for 1 hour at 100 °C, the solution was heated to 280 °C under Ar. After the solution turned clear, the solution was cooled to room temperature. Reheated the solution to a clear solution before the injection.^{1,2}

(5) Mn precursor (Mn acetate in OAm) for shell doping. OAm (8 mL) was added into a three-neck flask and degassed at room temperature for 10 minutes followed by degassing at 120 °C for additional 10 minutes. 7 mg (0.04 mmol) anhydrous Mn (CH₃CO₂)₂ was quickly added into the flask at room temperature. After degassing at room temperature for 10 minutes and an additional 10 minutes at 120 °C, the solution was cooled to room temperature.^{1,2} Note: The Mn precursor solution should be freshly made just before the injection.

Synthesis of Mn core-doped Mn:CdS and Mn:CdS/CdZnS/ZnS core/multi-shell QDs.

Mn(II) doped CdS QDs were synthesized through a colloidal hot-injection technique as previously described.¹ Briefly, 41.2 mg (0.130 mmol) of Cd (NO₃)₂·4H₂O, 5.82 mg (0.033 mmol) of Mn(NO₃)₂·H₂O, 0.167 mL of DDT, and 10 mL of OAm were mixed in a three-neck flask. The mixture was degassed for 40 min at room temperature and another 10 min at 100 °C. The mixture was refilled with Ar and kept at 110 °C for 30 min. Then, 0.667 mL of a 0.2 M solution of sulfur in OAm was swiftly injected into the flask when the mixture was

heated to 160 °C. After the injection, the temperature was set at 120 °C and degassed for 10 min. The temperature was then raised to 240 °C for nanocrystal growth for 5-10 min. The reaction was quenched by removing the heating mantle and submerging the flask in a cold-water bath. After the reaction had been cooled below 100 °C, the product was dissolved in toluene and then crashed out by adding ethanol. The QDs were separated from solutions by centrifugation with a speed set to 5000 rpm at 15 °C for 5 min. The supernatant was discarded and the QDs in the precipitant were redissolved in toluene or hexane, and the cleaning process was repeated 3 more times before shell coating.

A Successive Ion Layer Adsorption and Reaction (SILAR) procedure was used to synthesize core/multi-shell QDs.^{1,2} The as cleaned Mn:CdS core QDs were dissolved in ~1 mL hexane and then transferred into a new three-neck flask with 6 mL of ODE and 2 mL of OAm. After degassing at 90 °C for 30 minutes, the solution was heated to 100 °C, and continued to degas for another 10 minutes. Next, the solution was refilled with Ar, then the temperature was increased to 180 °C for the following shell growth. For the first CdZnS shell growth, the sulfur-precursor is dropwise injected by the Cd/Zn-precursor alternatively by the volume needed for 1 monolayer (ML) shell. For the following ZnS shell coating, alternating injections of the sulfur-precursor and the zinc-precursor were performed until the desired number of MLs was reached. A 10 °C increment of the reaction temperature was used after each ML shell growth throughout the multi shell growth procedure.

The QDs were cleaned once using toluene/ethanol and redissolved in toluene for optical measurements. For TEM, XRD, and EPR measurements, 4-6 additional washes using toluene/ethanol was performed.

Synthesis of Mn shell-doped core/multi-shell QDs.

For **CdS/CdZnS/Mn:ZnS/ZnS core/multi-shell QDs with Mn doped into ZnS shell**, the as-cleaned CdS core QDs were dissolved in ~1 mL hexane and then transferred into a new three-neck flask with 6 mL of ODE and 2 mL of OAm. After degassing at 90 °C for 30 minutes, the solution was heated to 100 °C, and degassed for another 10 minutes. Next, the solution was refilled with Ar, then the temperature was increased to 180 °C for the following shell growth using a SILAR procedure.^{1,2} For the first CdZnS shell growth, the sulfur-precursor was dropwise injected by the Cd/Zn-precursor alternatively by the volume needed for 1 ML shell. The Mn-Zn-precursor was injected dropwise for the Mn:ZnS shell. The CdS/CdZnS/Mn:ZnS QDs were cleaned using toluene/acetone to remove unreacted Mn and shell precursors and the cleaned QDs were transfer into a new three-neck flask for the following ZnS shell coating. For the following ZnS shell coating, alternating injections of the sulfur-precursor and the zinc-precursor were performed until the desired number of MLs was reached. A 10 °C increment of the solution temperature occurred after each ML shell growth throughout the multi shell growth procedure.

For the synthesis of the **CdS/CdZnS/Mn:CdS/ZnS core/multi-shell QDs with Mn doped into CdS shell**, the same procedure using the SILAR method was used except the Mn doped CdS layer was grown in the second shell by dropwise injecting the mixture of CdO and Mn-precursor. For control experiments without CdZnS alloyed trap layer, a CdS or ZnS layer was grown to replace the CdZnS layer in **CdS/CdS/Mn:CdS/ZnS** and **CdS/ZnS/Mn:ZnS/ZnS core/multi-shell QDs**, respectively. The same sample purification method was adopted for the shell doped core/multi-shell QDs as for the Mn core-doped core/multi-shell QDs.

Calculations for the Injections.

SILAR shell growth depends on adjusting the volume of the injection solution during the successive shell coating. The size and number of surface atoms of the QDs were used to calculate the amount of the metal ion precursor and sulfur precursor needed to grow 1 ML shell (larger volume shell precursor needed to grow 1 ML shell for QDs with larger diameters). The volume of alternating cationic and anionic solutions for the overcoating of CdZnS, CdS, ZnS shell in the core/multi-shell QDs are precisely injected into the reaction to get the theoretical thickness of each shell. The average thickness of each ZnS was considered to be 0.27 nm, so the diameter of the QDs after addition of each shell should increase ~ 0.54 nm.³

Characterizations.

Sample size, morphology, and dispersity were analyzed by transmission electron microscopy (TEM) using a JEOL JEM-2100F TEM which was operated at 200 kV. Powder X-ray diffraction (XRD) patterns were taken on a Bruker D2 Phaser with a LYKXEYE 1-dimensional silicon strip detector using Cu K α radiation ($\lambda = 1.5406$ Å). The elemental analysis of the samples was conducted by a PerkinElmer Avio-220 Max inductively coupled plasma-optical emission spectrometry (ICP-OES). For ICP-OES measurements, the powdered samples were completely dissolved in 65% HNO₃, heated to remove excess NO_x, and then diluted with 2% HNO₃ solution.

Agilent Cary 60 UV-vis spectrophotometer was used to collect absorption spectra of the samples in a 1 cm quartz cell. PL measurements were conducted with a Horiba FluoroMax Plus spectrofluorometer. Time-resolved emission measurements were performed using an Edinburgh FLS-980 fluorescence spectrometer equipped with 365 nm picoseconds pulsed lasers (EPLSs) and microsecond flashlamp (μF_2) to measure PL lifetime from a few nano seconds to seconds. Room temperature EPR spectra was performed by a Bruker ELEXSYS-II E500 spectrometer with a microwave frequency of 9.7 GHz.

Quantum chemical calculations.

All quantum chemical calculations were performed using density functional theory (DFT) using the B3LYP functional using LANL2Z basis set and LANL effective core potentials. The tetrahedral (T_d) sites occupied by Mn(II) for ZnS and CdS lattice were obtained from the respective crystal structures. The minimum-energy path (MEP) for dopant migration from an occupied T_d site to an adjacent vacant T_d site was calculated using the TERACHEM quantum chemistry package which was then used to calculate the energy barrier for the dopant migration.

II. Controlled outward dopant migration in Mn core-doped core/multi-shell QDs.

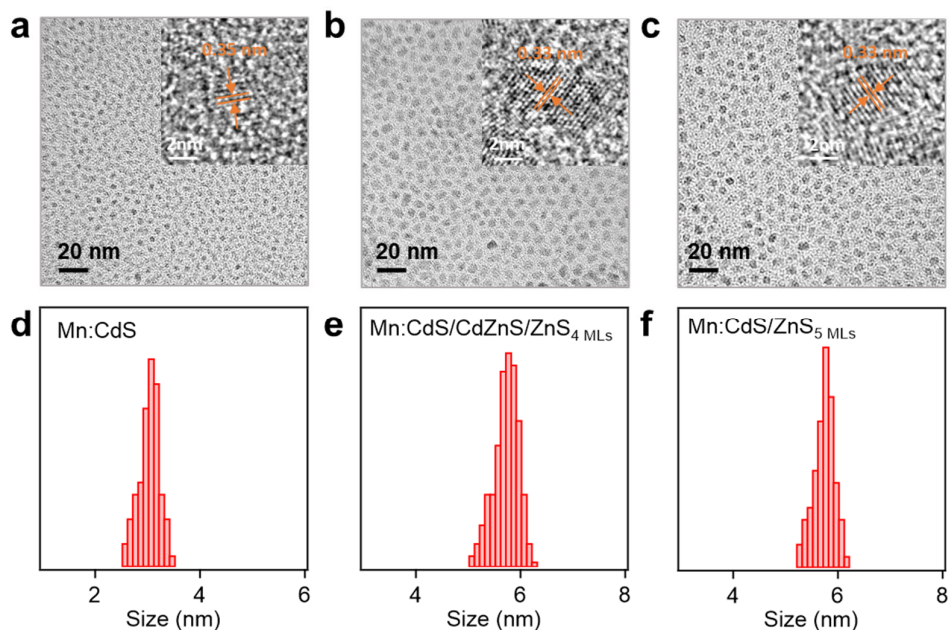


Figure S1. TEM Images and histogram of selected (a and d) Mn:CdS core QDs, (b and e) Mn:CdS/CdZnS/ZnS₄ MLs core/multi-shell QDs, (c and f) Mn:CdS/ZnS₅ MLs core/shell QDs. The insets are the high-resolution TEM images showing d-spacing of the (111) lattice plane of the corresponding QDs.

The size of the Mn:CdS core QDs is 3.0 ± 0.3 nm. For Mn:CdS/ZnS₅ MLs core/shell QDs, 5 MLs of ZnS were coated onto the Mn:CdS core with a final size of 5.7 ± 0.3 nm. For Mn:CdS/CdZnS/ZnS₄ MLs core/multi-shell QDs, 1 ML of CdZnS and 4 MLs of ZnS were coated onto the Mn:CdS core with the size of the QDs of 5.6 ± 0.3 nm after shell growth.

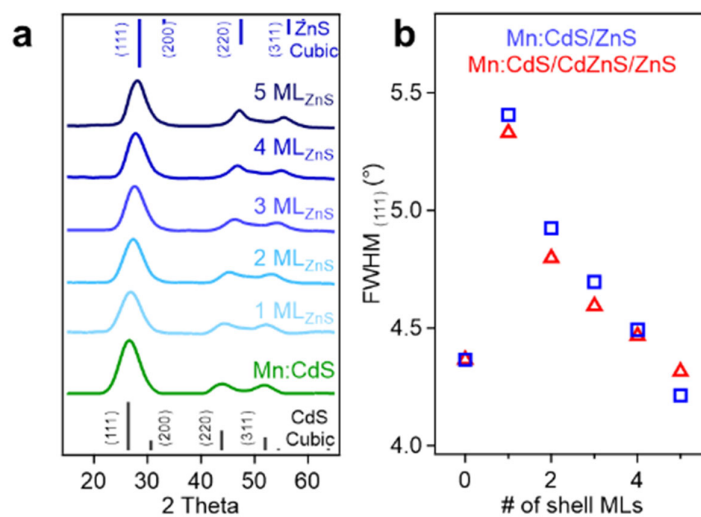


Figure S2. (a) XRD patterns of Mn:CdS/ZnS core/shell QDs. (b) XRD analysis of full width at half maximum (FWHM) of the (111) diffraction peak of the Mn:CdS/ZnS and Mn:CdS/CdZnS/ZnS core/multi-shell QDs as a function of the shell thickness.

Calculation of the average distance between Mn ions within QDs before and after dopant migration.

For the Mn core-doped CdS QDs, we first calculated the volume (V) of a QD using the equation 1,

$$V = \frac{4}{3}\pi r^3 \quad (\text{Eq. 1})$$

Where r is the radius of a spherical Mn:CdS QD.

From the Mn doping concentration, we can obtain the number of Mn ions per QD (n). Therefore, the average volume occupied by each Mn ion in the Mn:CdS QDs (V_{Mn}) is:

$$V_{Mn} = \frac{V}{n} = \frac{\frac{4}{3}\pi r^3}{n} = \frac{4}{3}\pi r_{Mn}^3 \quad (\text{Eq. 2})$$

Therefore, the radius of a sphere of Mn ion (r_{Mn}) occupied is:

$$r_{Mn} = \sqrt[3]{\frac{V_{Mn}}{\frac{4}{3}\pi}} \quad (\text{Eq. 3})$$

Using equation 1 to 3, the average Mn-Mn distance in the Mn:CdS QD could be estimated as $2 * r_{Mn}$.

After dopants outward migration toward the alloyed layer in Mn:CdS/CdZnS/ZnS and Mn:CdS/ZnS QDs, Mn ions would occupy in a thin shell layer above the CdS core. The surface area of a Mn:CdS/CdZnS_(1ML) QD or a Mn:CdS/ZnS_(1ML) QD can be calculated using Eq. 4,

$$A_{shell} = 4\pi r_{QD}^2 \quad (\text{Eq. 4})$$

The average area occupied by each Mn ion can be calculated using Eq 5. It should be noted that decreased doping concentration after shell coating and the number of Mn ions per core/shell QD is represented as n'.

$$A_{Mn} = A_{shell}/n' \quad (\text{Eq. 5})$$

The radius of the circle occupied by a Mn ion (R_{Mn}) is,

$$R_{Mn} = \sqrt{\frac{A_{Mn}}{4\pi}} \quad (\text{Eq. 6})$$

Then the average Mn-Mn distance in the shell can be estimated as $2 * R_{Mn}$.

For the Mn shell-doped CdS/CdZnS/Mn:CdS/ZnS core/multi-shell QDs with inward dopant migration, we use the Eq. 4-6 to calculate the average Mn-Mn distance in the original CdS shell and CdZnS shell after dopant inward migration.

We summarized the results for the core doped core/shell QDs (outward migration) in the Table 1 and Table 2, and the shell doped core/multi-shell QDs (inward migration) in the Table 3.

Table S1. The average distance between Mn ions inside Mn:CdS core QDs.

Sample	[Mn]	Number of Mn ions per QD (n)	Average volume occupied by Mn ions (V) /nm ³	Average volume occupied per Mn ion (V_{Mn}) /nm ³	Average distance between Mn ions (d_{Mn}) /nm
Mn:CdS	1.2%	6	14.14	2.36	1.65

Table S2. The average distance between Mn ions inside Mn:CdS/CdZnS QDs and Mn:CdS/ZnS QDs with outward dopant migration behavior.

Sample	[Mn]	Number of Mn ions per QD (n)	Assuming dopant radial position from the center of a QD/nm	Average surface area occupied per Mn ion (A_{Mn}) /nm ²	Average distance between Mn ions (d_{Mn}) /nm
Mn:CdS/ CdZnS	0.9%	4	At the core/shell interface (1.5 nm)	7.07	1.50
			At the midpoint of CdZnS shell (1.63 nm)	8.30	1.63
			At the outer surface of CdZnS shell layer (1.75 nm)	9.62	1.75
Mn:CdS/ ZnS _(1 ML)	0.6%	3	At the core/shell interface (1.5 nm)	9.42	1.73
			At the midpoint of ZnS shell (1.63 nm)	11.06	1.88
			At the outer surface of ZnS shell layer (1.75 nm)	12.83	2.02

Note: ZnS shell coated Mn:CdS/CdZnS QDs, *i.e.* Mn:CdS/CdZnS/ZnS_(1-4 MLs), have the same dopant concentration, and therefore the same average distance between Mn ions, regardless of the ZnS shell MLs.

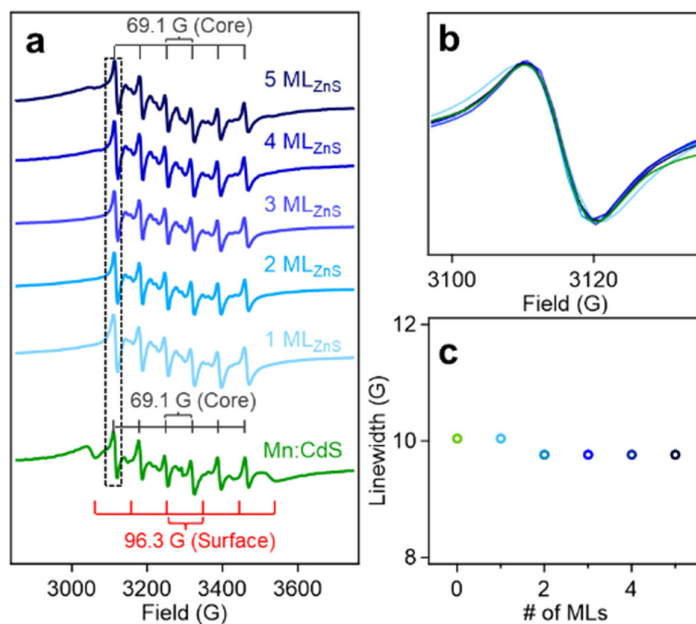


Figure S3. (a) Room Temperature X-Band EPR spectra of Mn:CdS/ZnS_(1-5 MLs) core/shell QDs. Two discrete sites for the Mn(II) occupied a substitutional Cd(II) site within the CdS core (hyperfine splitting constant A is 69.1 G) and surface ($A = 96.3$ G). During the shell passivation, only the core site, hyperfine splitting constant $A = 69.1$ G was observed. (b) The representative first sextet hyperfine peak of EPR spectra to display slightly decreasing spectral linewidth and (c) the EPR spectra linewidth as a function of shell monolayers.

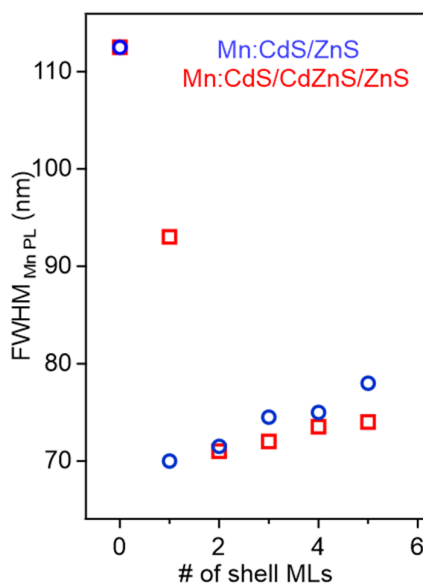


Figure S4. FWHM of Mn PL peak for Mn:CdS/ZnS_(1-5 MLs) and Mn:CdS/CdZnS/ZnS_(1-4 MLs) core/multi-shell QDs.

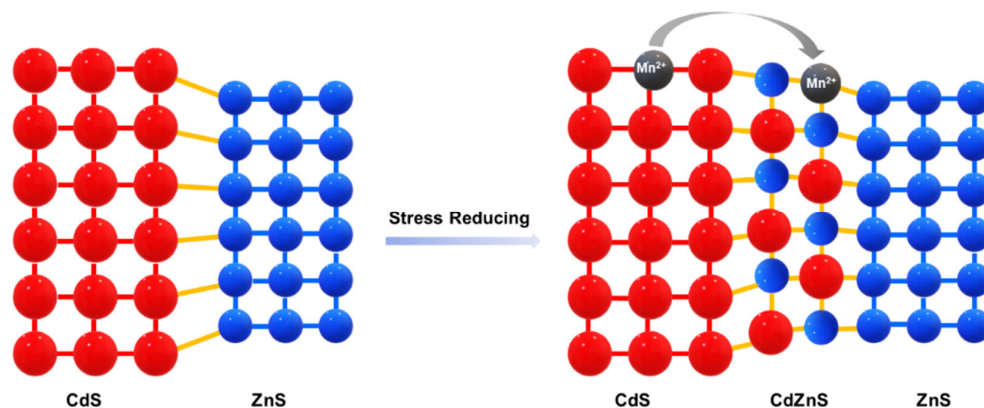


Figure S5. Schematic of inserting an alloyed CdZnS layer to reduce the lattice strain between CdS and ZnS lattice.

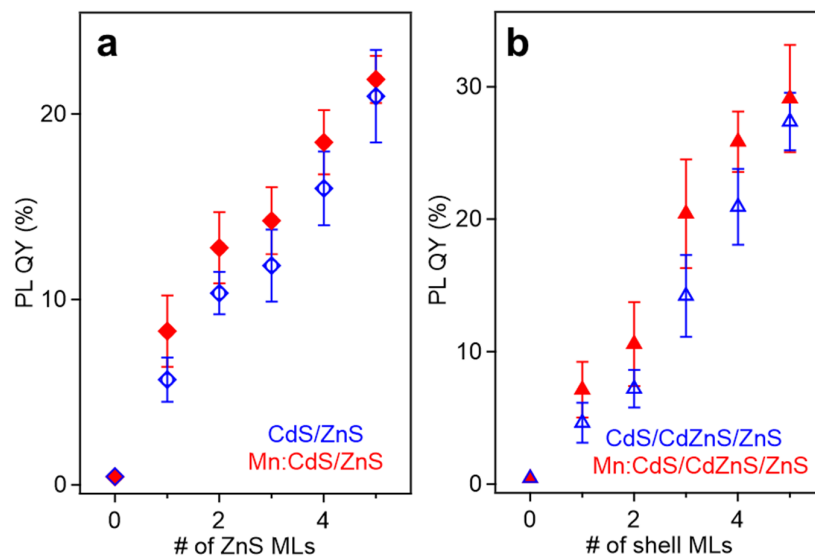


Figure S6. PL QYs of (a) undoped CdS/ZnS_(1-5 MLs) and doped Mn:CdS/ZnS_(1-5 MLs) core/multi-shell QDs without an inserted alloy dopant trap, and (b) undoped CdS/CdZnS/ZnS_(1-4 MLs) and doped Mn:CdS/CdZnS/ZnS_(1-4 MLs) core/multi-shell QDs with an inserted CdZnS alloy dopant trap as a function of ZnS monolayers, respectively.

III. Controlled inward dopant migration in Mn shell-doped core/multi-shell QDs.

Mn ion doping into ZnS shell with smaller initial substitutional Zn sites.

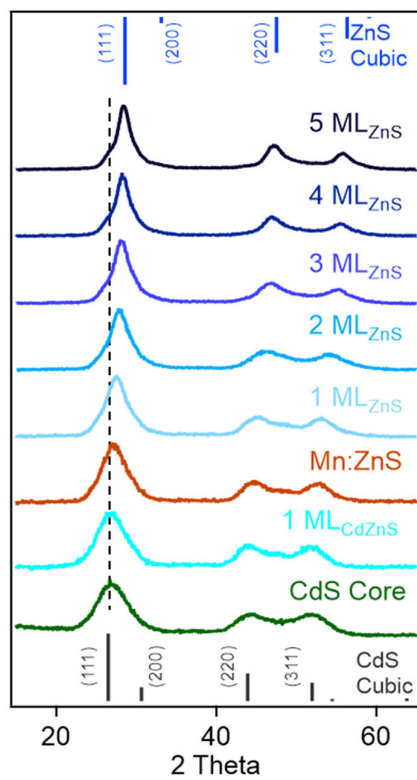


Figure S7. XRD patterns of CdS core and CdS/CdZnS/Mn:ZnS/ZnS_(1-5 MLs) core/multi-shell QDs.

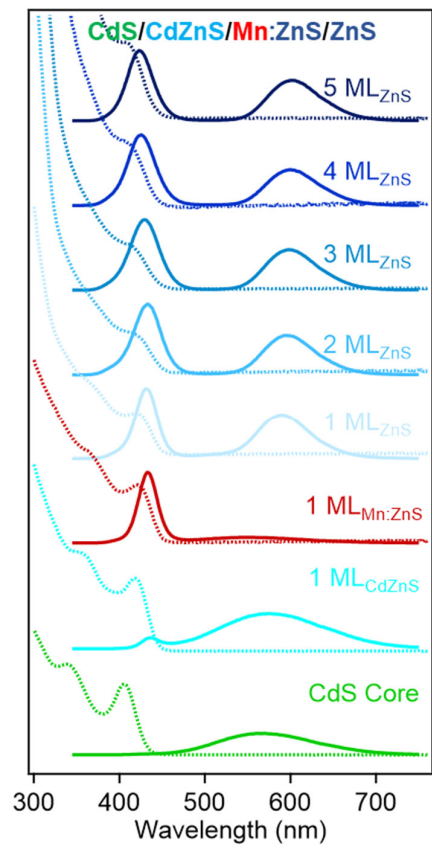


Figure S8. Normalized absorption (dotted lines) and PL (solid lines) spectra of CdS core and CdS/CdZnS/Mn:ZnS/ZnS_(1-5 ML_s) core/multi-shell QDs.

Mn ion doping into CdS shell with larger initial substitutional Cd sites.

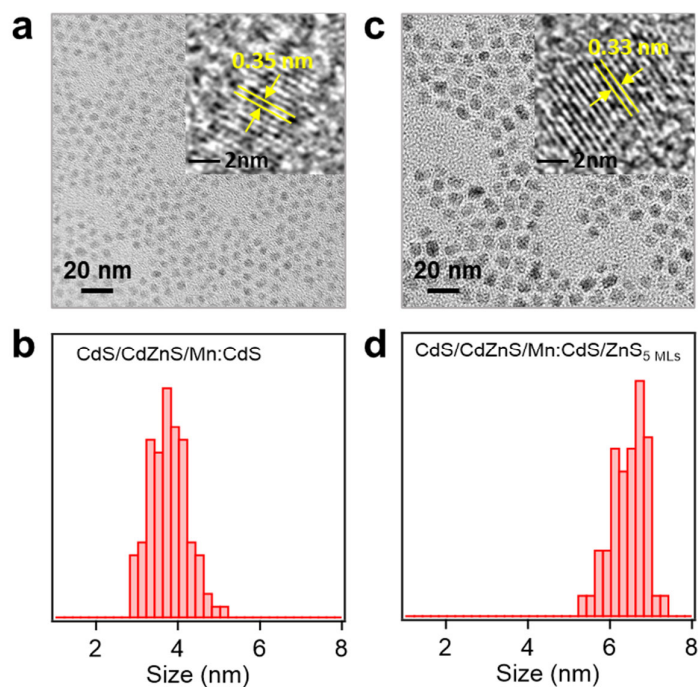


Figure S9. TEM Images and histogram of CdS/CdZnS/Mn:CdS and CdS/CdZnS/Mn:CdS/ZnS₅ MLs core/multi-shell QDs. The insets are the high-resolution TEM images showing d-spacing of the (111) lattice plane of the QDs. The slight decrease in the average interplanar spacing from 0.35 nm of CdS/CdZnS/Mn:CdS to 0.33 nm of CdS/CdZnS/Mn:CdS/ZnS₅ MLs core/multi-shell QDs is consistent with the smaller lattice parameters of ZnS compared with that of CdS. The size of the QDs increased from 3.8 ± 0.3 nm (a and b) to 6.4 ± 0.3 nm (c and d) for 5 MLs of ZnS shell coated on the QDs.

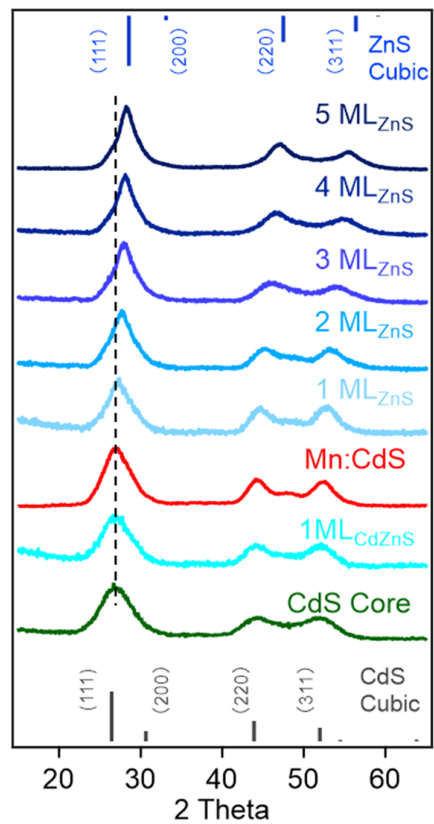


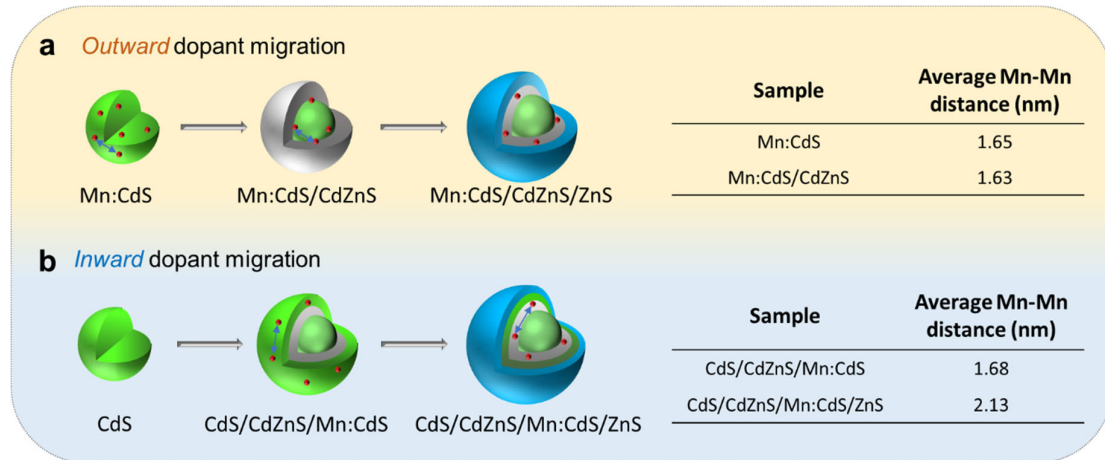
Figure S10. XRD patterns of CdS/CdZnS/Mn:CdS/ZnS core/multi-shell QDs as a function of shell thickness.

Table S3. The average distance between Mn ions inside CdS/CdZnS/Mn:CdS QDs and CdS/CdZnS/Mn:CdS/ZnS QDs with inward dopant migration behavior.

Sample	[Mn]	Number of Mn ions per QD (n)	Assuming dopant radial position from the center of a QD/nm	Average surface area occupied per Mn ion (A_{Mn})/nm ²	Average distance between Mn ions (d_{Mn})/nm
CdS/CdZnS/ Mn:CdS	0.4%	5	At the CdZnS and Mn:CdS shell interface (1.75 nm)	7.70	1.57
			At the midpoint of Mn:CdS shell (1.88 nm)	8.84	1.68
			At the outer surface of Mn:CdS shell layer (2 nm)	10.04	1.79
CdS/CdZnS/ Mn:CdS/ ZnS _{1ML}	0.3%	4	At the CdZnS and Mn:CdS shell interface (2 nm)	12.57	2.00
			At the midpoint of Mn:CdS shell (2.13 nm)	14.19	2.13
			At the to outer surface of Mn:CdS shell layer (2.25 nm)	15.90	2.25

Note: ZnS shell coated CdS/CdZnS/Mn:CdS QDs, *i.e.*, CdS/CdZnS/Mn:CdS/ZnS_(1-5 MLs), have the same dopant concentration, and therefore the same average distance between Mn ions, regardless of the ZnS shell MLs.

Scheme S1. Average Mn-Mn distance before and after both outward and inward dopant migration inside core- and shell-doped QDs, respectively.



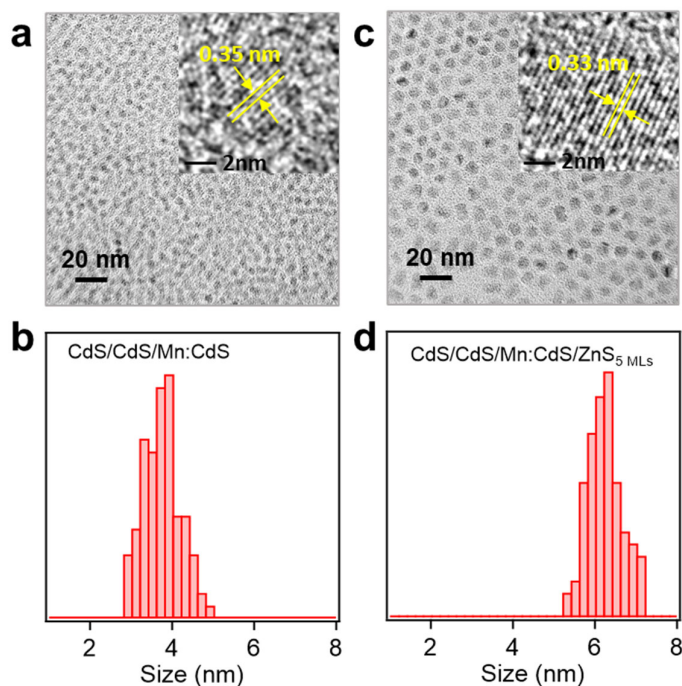


Figure S11. TEM Images and histogram of CdS/CdS/Mn:CdS and CdS/CdS/Mn:CdS/ZnS₅ MLs core/multi-shell QDs. The insets are the high-resolution TEM images showing d-spacing of the (111) lattice plane of the QDs. The slight decrease in the average interplanar spacing from 0.35 nm of CdS/CdS/Mn:CdS to 0.33 nm of CdS/CdS/Mn:CdS/ZnS₅ MLs core/multi-shell QDs is consistent with the smaller lattice parameters of ZnS compared with that of CdS. The size of QDs increased from 3.8 ± 0.3 nm (a and b) to 6.4 ± 0.3 nm (c and d) for 5 MLs of ZnS shell coated on the QDs.

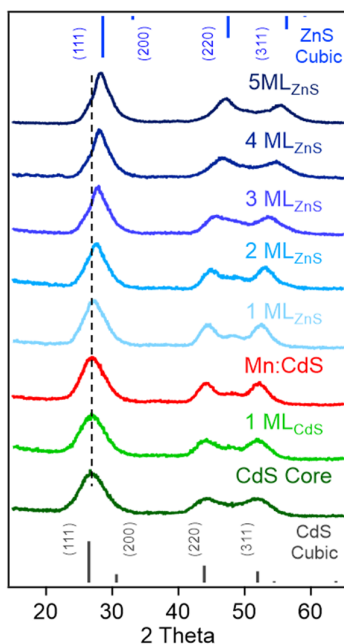


Figure S12. XRD patterns of CdS/CdS/Mn:CdS/ZnS core/multi-shell QDs as a function of shell thickness.

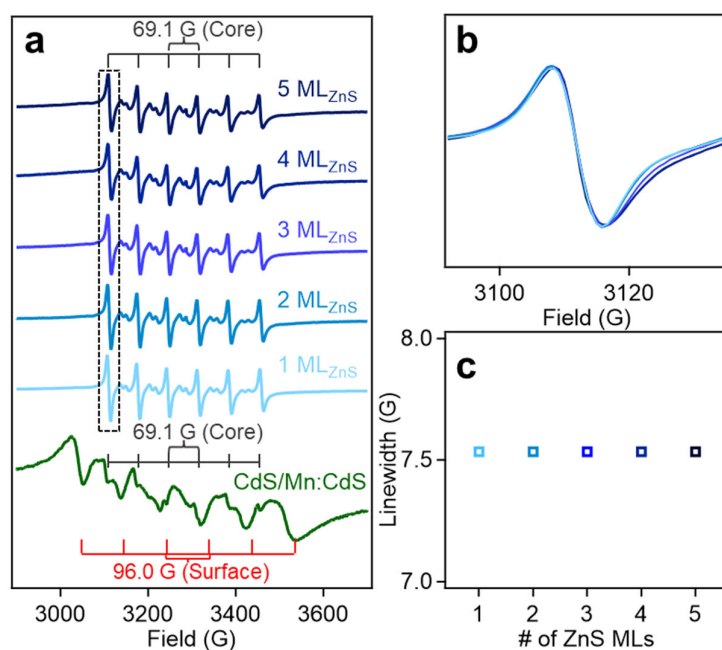


Figure S13. (a) Room Temperature X-Band EPR spectra of CdS/CdS/Mn:CdS/ZnS_(1-5 MLs) core/multi-shell QDs. Two discrete substitutional Mn(II) sites including the core Mn(II) sites (hyperfine splitting constant (A): 69.1 G) and surface Mn(II) sites (A: 96.0 G). During the shell passivation, only the core site (A = 69.1 G) was observed. (b) The representative first sextet hyperfine peak of EPR spectra to display spectra linewidth and (c) the EPR hyperfine peak linewidth as a function of shell monolayers.

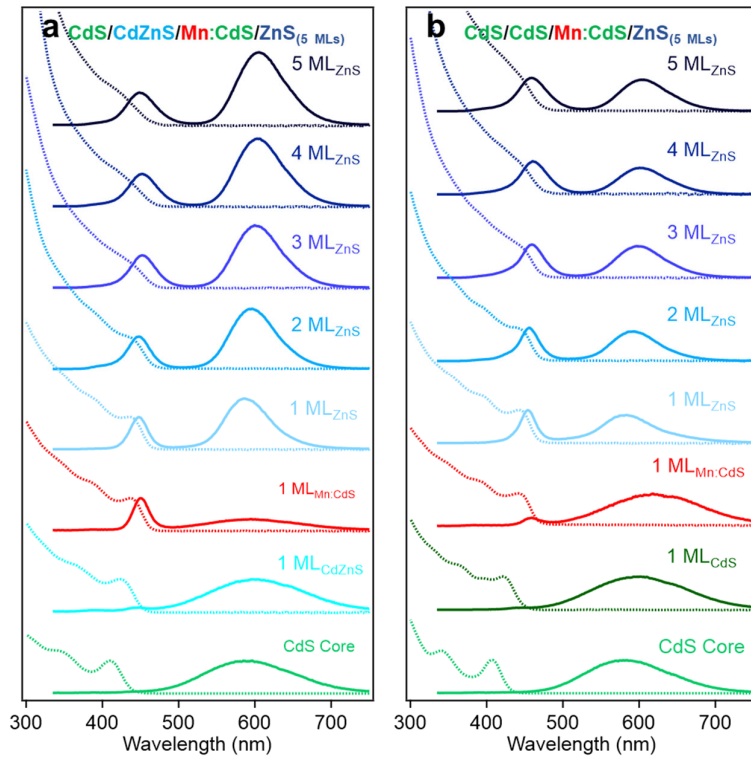


Figure S14. Normalized absorption (dotted lines) and PL (solid lines) spectra of (a) CdS/CdZnS/Mn:CdS/ZnS_(1-5 MLs) and (b) CdS/CdS/Mn:CdS/ZnS_(1-5 MLs) core/multi-shell QDs.

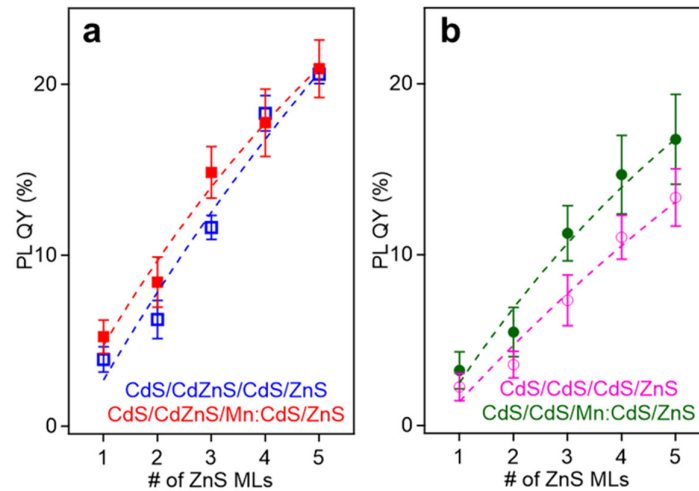


Figure S15. PL QYs (a) shell doped CdS/CdZnS/Mn:CdS/ZnS_(1-5 MLs) and undoped CdS/CdZnS/CdS/ZnS_(1-5 MLs) core/multi-shell QDs, and (b) shell doped CdS/CdS/Mn:CdS/ZnS_(1-5 MLs) and undoped CdS/CdS/CdS/ZnS_(1-5 MLs) core/multi-shell QDs.

Author Contributions

W.Z. directed the project. C.C. and W.Z. conceived and designed the project. C.C. and E.H. performed all the experiments. C.G. and A.C. performed DFT calculations. S.L., H.L., and W.M. assisted in TEM and XRD experiments. J.M.F. and R.W.M. assisted in EPR measurements and analysis. C.C. and W.Z. co-wrote the manuscript. All authors discussed the results and commented on the manuscript.

References:

1. E. Hofman, R. J. Robinson, Z. J. Li, B. Dzikovski and W. Zheng, Controlled dopant migration in CdS/ZnS core/shell quantum dots, *J. Am. Chem. Soc.*, 2017, **139**, 8878-8885.
2. Y. Yang, O. Chen, A. Angerhofer and Y. C. Cao, On doping CdS/ZnS core/shell nanocrystals with Mn, *J. Am. Chem. Soc.*, 2008, **130**, 15649-15661.
3. J. J. Li, Y. A. Wang, W. Guo, J. C. Keay, T. D. Mishima, M. B. Johnson and X. Peng, Large-scale synthesis of nearly monodisperse CdSe/CdS core/shell nanocrystals using air-stable reagents via successive ion layer adsorption and reaction, *J. Am. Chem. Soc.*, 2003, **125**, 12567-12575.